RSC Advances

PAPER

View Article Online
View Journal | View Issue

Cite this: *RSC Adv.*, 2021, **11**, 32740

NS3/4A helicase inhibitory alkaloids from *Aptenia cordifolia* as HCV target†

Asmaa Abo Elgoud Said,[a] Ahmed H. Afifi,[b] Taha F. S. Ali,[c] Mamdouh Nabil Samy,[a] Usama Ramadan Abdelmohsen,*[ad] Mostafa A. Fouad[a] and Eman Zekry Attia[a]

Received 13th August 2021
Accepted 29th September 2021

DOI: 10.1039/d1ra06139a

rsc.li/rsc-advances

Chemical investigation of *Aptenia cordifolia* roots extract, using chromatographic and spectroscopic techniques, resulted in isolation and identification of eight known compounds. The basic ethyl acetate fraction (alkaloidal fraction) afforded *O*-methylsceletenone, epinine, 4-methoxy phenethylamine, and *N*-methyl tyramine while, the acidic ethyl acetate fraction (non-alkaloidal fraction) afforded only *cis*-*N*-coumaroyl tyramine. Moreover, the petroleum ether fraction afforded capric acid, tricosanol, and a mixture of β-sitosterol & stigma sterol. Upon screening of anti HCV activity of these three fractions, only the basic ethyl acetate fraction had high activity against HCV with an IC_{50} value equal to 2.4 μg mL^{-1} which provoked us to carry out structure based *in silico* virtual screening on the drug targets of HCV of isolated alkaloidal compounds as well as the previously dereplicated alkaloids through metabolomics from the antiviral active fraction. The tortuosamine compound exhibited the strongest binding to the active site of NS3/4A helicase with a binding affinity (−7.1 kcal mol^{-1}) which is very close to the native ligand (−7.7 kcal mol^{-1}).

1. Introduction

Hepatitis C virus (HCV) was first identified in 1989.[1] It is an enveloped, positive stranded RNA virus belonging to the family Flaviviridae and considered to be a public health concern which infects more than 185 million people worldwide.[2,3] HCV is the major etiological agent of non-A non-B hepatitis as the infection occurs principally through blood or blood-derived products.[4] This viral infection is the leading cause of cirrhosis and, as a result, liver transplantation around the world.[5,6] The conventional HCV treatment has advanced quickly, as several protease inhibitors, such as boceprevir and telaprevir have recently been recommended as hepatitis C therapy. These novel inhibitors, however, have been linked to drug toxicity, the creation of resistance mutants, high cost and efficacy limitation.[7] Indeed, the challenge is to develop a potent, inexpensive and widely available antiviral drug.

Medicinal plants contain a variety of compounds that have the potential to treat ailments, particularly infectious disorders. Different studies declared beneficial effects of secondary metabolites derived from medicinal plants against viral diseases. A broad variety of these secondary metabolites, such as alkaloids, coumarins, lignans and polyphenolic compounds affect cellular functions and replication of various infectious viruses. Medicinal plants' history dates back to the origin of human civilization on this planet. Inhibitory activity of medicinal plants extracts against replication of several viruses was reported latterly, such as, herpes simplex virus type2 (HSV-2),[8] HIV,[9,10] hepatitis B virus (HBV),[11,12] emerging viral infections associated with poxvirus, and severe acute respiratory syndrome (SARS) virus.[13] Recently, various studies have been conducted to investigate the antiviral activity of a variety of plants. As the methanolic extract of both *Terminalia bellerica* seeds and *Enicostemma axillare* showed antiviral activity against hepatitis B.[14] On the other hand, *Stixis scandens* Lour leafe extract showed powerful antiviral activity against porcine epidemic diarrhea virus.[15] Moreover, silymarin, epigallocatechin gallate, naringenin,[16] phenolic compounds of grape seed and aqueous extract of Eclibta alba leaves exhibited anti HCV activity.[14] The alcoholic and/or water soluble extracts of medicinal plants were utilized during furthermost of these antiviral studies. Genus *Aptenia* is endemic to South Africa and includes four species, which are currently recognized as *Aptenia cordifolia* L.F. Schwantes, *Aptenia geniculiflora* L. Bittrich ex Gerbaulet, *Aptenia haeckeliana* A. Berger Bittrich ex Gerbaulet, and *Aptenia lancifolia* L. Bolus.[17] *Aptenia cordifolia*, a well-known

[a]*Department of Pharmacognosy, Faculty of Pharmacy, Minia University, 61519 Minia, Egypt. E-mail: usama.ramadan@mu.edu.eg; Fax: +20-86-2369075; Tel: +20-86-2347759*

[b]*Department of Pharmacognosy, Division of Pharmaceutical Industries, National Research Center, Dokki, 12622, Giza, Egypt*

[c]*Department of Medicinal Chemistry, Faculty of Pharmacy, Minia University, 61519 Minia, Egypt*

[d]*Department of Pharmacognosy, Faculty of Pharmacy, Deraya University, Universities Zone, 61111 New Minia City, Egypt*

† Electronic supplementary information (ESI) available. See DOI: 10.1039/d1ra06139a

groundcover, was named heart-leaved ice plant and has only one synonym "*Mesembryanthemum cordifolium*".[18] So as to provide a complementary therapy for previously existing remedies, the antiviral activity of different fractions (petroleum ether, acidic ethyl acetate and basic ethyl acetate) derived from the total ethanol extract of *A. cordifolia* roots were examined against HCV by *in vitro* cells culture using luciferase assay and the cytotoxic effect was accessed by MTT assay. Additionally, we aimed to identify which compound/s in the basic ethyl acetate fraction responsible for the anti HCV activity as well as the mechanism of action by undergoing docking studies on the drug targets of HCV. Although there are many HCV targets, our docking study will focus on the most attractive viral proteins required for HCV replication. These targets are NS5B HCV RNA-dependent RNA polymerase, NS3/4A protease, NS3/4A helicase, and a new allosteric pocket in the HCV NS3–NS4A protein located at the interface between the protease and helicase domains. The compounds used for docking studies were the isolated alkaloids from the active fraction (basic ethyl acetate fraction), as well as, the previously nine dereplicated alkaloids from the basic ethyl acetate fraction through metabolomic analysis.[19]

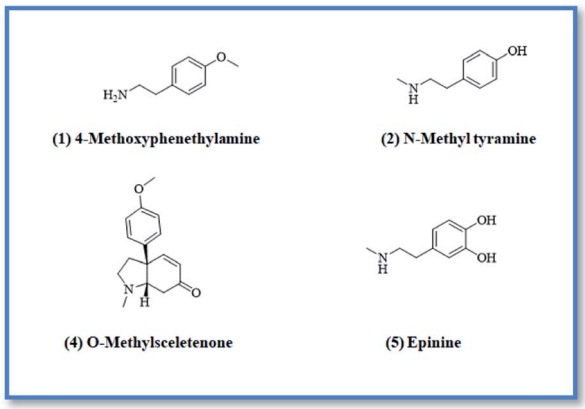

Fig. 1 Isolated compounds from alkaloidal fraction.

2. Results and discussion

2.1. Identification of the isolated compounds

The petroleum ether fraction afforded four compounds. Mixture of β-sitosterol & stigma sterol (8 mg) was isolated as white amorphous powder, and was simply identified by comparison with authentic sample. This mixture was previously isolated from the aerial parts of the plant.[20]

Tricosanol alcohol (5 mg) was isolated as white powder and the complete assignment was confirmed by investigation of ^{1}H-NMR, DEPT-Q and ESI-MS analyses. The molecular formula was determined to be $C_{23}H_{48}O$ by ESI-MS that showed a pseudo molecular ion peak at 339 $[M–H]^-$. The compound was identified by comparison of the ESI-MS and NMR data, with the reported data[21] and this is the first time for its isolation from family Aizoaceae.

Capric acid was isolated as white powder (4 mg), the molecular formula was confirmed to be $C_{10}H_{20}O_2$ by ESI-MS that showed a molecular ion peak at 172.8 $[M]^+$. The compound was identified by comparison of the ESI-MS and ^{1}H-NMR data with the reported data,[22] and it was previously identified by GC-MS in *Attalea dubia* family Arecaceae, but this is the first time for its isolation from family Aizoaceae.

Cis-N-coumaroyl tyramine (**3**),which was isolated as white powder (5 mg), HR-ESI-MS showed a pesudo molecular ion peak at *m*/*z* 284.128 $[M + H]^+$, (calculated mass at *m*/*z* 284.128) corresponding to the molecular formula $C_{17}H_{18}NO_3$ in addition to, a characteristic fragment peak at *m*/*z* 147.057 corresponding to loss of $[M–C_8H_{11}NO]$. It was identified by comparison ^{1}H-NMR

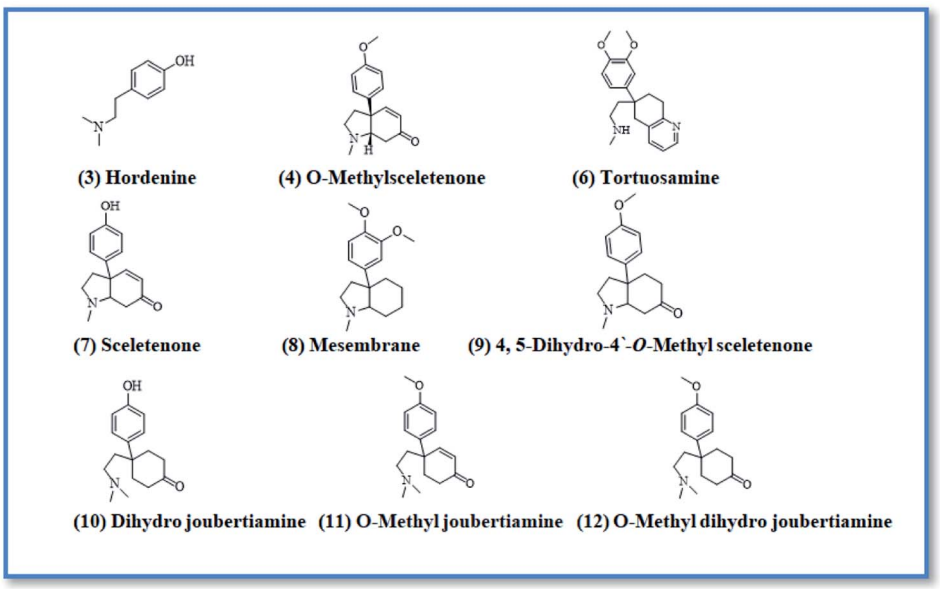

Fig. 2 Dereplicated compounds from alkaloidal fraction.

data with the literature,[23] and this is the first report for its isolation from family Aizoaceae.

4-Methoxyphenethylamine (**1**) was isolated as white powder (3 mg, purity 97%) HR-ESI-MS of compound **1** showed a pseudo molecular ion peak at *m*/*z* 152.1066 $[M + H]^+$ (calculated mas 152.1075), corresponding to the molecular formula $C_9H_{14}NO$. From the HR-ESI-MS, ^{1}H-NMR data and from the reported data in literature[24] compound **1** was identified as 4-methoxyphenethylamine which was previously isolated from *Coryphantha pectinata*[25] and this is the first report for its isolation from family Aizoaceae.

N-Methyltyramine (**2**) was isolated as white powder (4 mg). HR-ESI-MS of compound **2** showed a pseudo molecular ion peak at *m*/*z* 152.0697 $[M + H]^+$ (calculated mas 152.1031), corresponding to the molecular formula $C_9H_{14}NO$. From ESI-MS, ^{1}H-NMR data and from the data reported in literature[26] compound **2** was identified as *N*-methyltyramine which was previously isolated from *Sawa millet* seeds[26] and this is the first report for its isolation from family Aizoaceae.

O-methylsceletenone (**4**) was isolated as reddish brown powder (20 mg, purity 98%), the complete assignment of compound **4** was confirmed by investigation of ^{1}H-NMR, DEPT and HR-ESI-MS. Positive HR-ESI-MS of compound **4** showed a quassi molecular ion peak at *m*/*z* 258.1462 $[M + H]^+$, (calculated mass at *m*/*z* 258.1494) corresponding to the molecular formula $C_{16}H_{20}NO_2$. From the HR-ESI-MS, NMR data and in comparison with the literature,[27] compound **4** was identified as *O*-methyl sceletenone. It was previously isolated from different organs of the investigated plant.[28]

Epinine (**5**) was isolated as yellow powder (4 mg, purity 97%) HR-ESI-MS of compound **5** showed a pseudo molecular ion peak at *m*/*z* 168.9802 $[M + H]^+$, (calculated mass at *m*/*z* 167.1024) corresponding to the molecular formula $C_9H_{14}NO_2$. Comparison of the HR-ESI-MS and ^{1}H-NMR data of compound **5**, with the data reported in literature[29,30] revealed that compound **5** is epinine alkaloid which was previously isolated from *Cytisus scoparius* Family Leguminosae[31] and this is the first report for its isolation from family Aizoaceae.

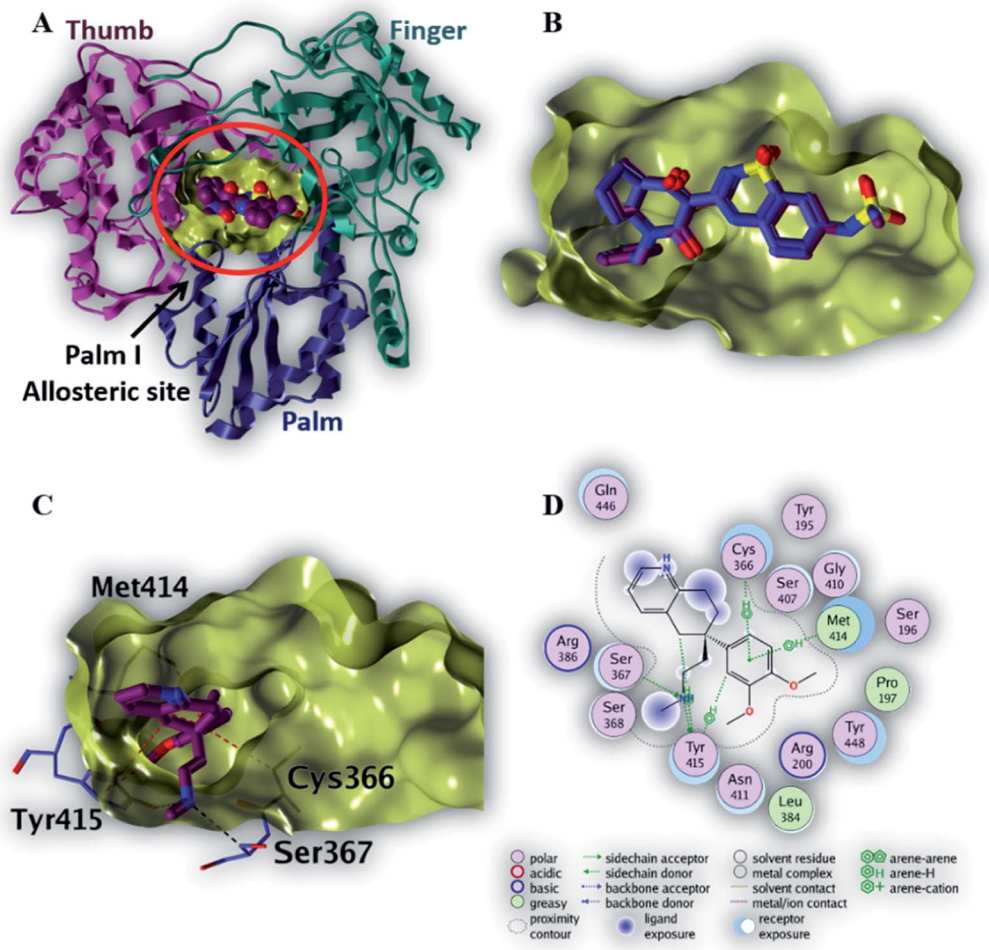

Fig. 3 The top-scoring docked pose of compound **6** to the HCV NS5B polymerase active site (PDB code: 3H2L) as predicted by MOE 2019.01. (A) An overview of the HCV NS5B polymerase active site (B) comparison of modeled binding mode of the co-crystallized ligand (a novel bicyclic dihydro-pyridinone inhibitor) (magenta stick model) and its superposed docking conformation (blue stick model). (C) Detailed binding mode of compound **6** (magenta stick model) displaying hydrogen bonds (black dashed line) and H–π interactions (red dashed line) with the key amino acid residue (blue stick model). (D) 2D depiction of compound **6** binding interactions with the critical amino acid residue.

2.2. Antiviral activity and molecular docking simulation

Upon screening the HCV antiviral activity of different fractions of *A. cordifolia* roots extract, only the basic ethyl acetate fraction (alkaloidal fraction) displayed high potential against HCV with IC_{50} value equal to 2.4 μg mL^{-1}. According to the HCV genome, there are four structural (core, E1, E2, and p7) and six non-structural (NS2, NS3, NS4A, NS4B, NS5A, and NS5B) proteins.[32,33] The non-structural proteins that accounted for viral production and replication are the primary targets for the currently FDA-approved drugs designed against HCV.[34] In addition, there is a newly discovered binding pocket between the protease and helicase domains, also considered a druggable target. Of the six non-structural viral proteins, NS2/3 autoprotease, which mediates a single cleavage in the polyprotein, has been less well explored. Moreover, the NS5A protein, involved in both RNA replication and infectious virus assembly, is not a promising target because it has no known enzymatic activity.[35] Therefore, our main target is *in silico* prediction of the binding affinities of the four alkaloids isolated from the alkaloidal fraction of the *A. cordifolia* roots named, 4-methoxyphenethylamine (**1**), *N*-methyl tyramine (**2**), *O*-methylsceletenone (**4**) and epinine (**5**) (Fig. 1) as well as previously reported nine alkaloids dereplicated from alkaloidal fraction through metabolomic analysis (**3** and **6–12**) (Fig. 2)[19] against the four non-structural HCV antiviral targets: namely NS5B HCV RNA-dependent RNA polymerase, NS3/4A protease, NS3/4A helicase, and a new allosteric pocket in the HCV NS3–NS4A protein located at the interface between the protease and helicase domains.

Before docking of the screened compounds, we assessed our MOE induced docking protocol by re-docking the co-crystallized ligand within the active site of NS5B HCV RNA-dependent RNA polymerase (PDB code: 3H2L), NS3/4A protease (PDB code: 6NZT), NS3/4A helicase (PDB code: 4OKS), and a new allosteric

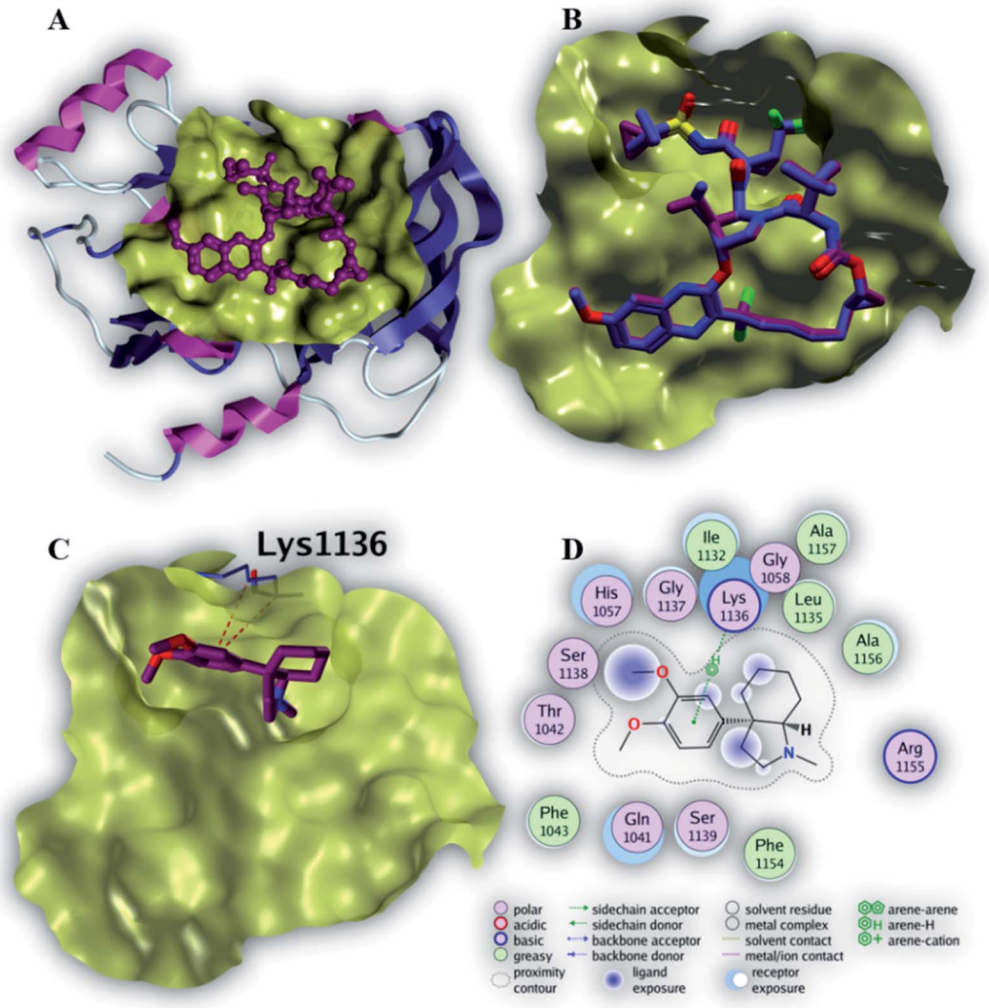

Fig. 4 The top-scoring docked pose of compound **8** to the HCV NS3/4A protease active site (PDB code 6NZT) as predicted by MOE 2019.01. (A) An overview of the HCV NS3/4A protease active site (B) comparison of modeled binding mode of the co-crystallized ligand Voxilaprevir (magenta stick model) and its superposed docking conformation (cyan stick model). (C) Detailed binding mode of compound **8** (green stick model) displaying H–π bond (red dashed line) with the key amino acid residue (cyan stick model). (D) 2D depiction of compound **8** binding interactions with the key amino acid residue.

pocket in the HCV NS3–NS4A protein located at the interface between the protease and helicase domains (PDB code: 4B73).

As seen in Fig. 3–6, MOE successfully re-docked the native ligand in its original pose with acceptable RMSD values of 0.28, 0.62, 0.31, and 0.16 Å respectively. The binding free energies of the re-docked ligand, as well as the screened compounds, were summarized in Table 1.

Among the screened compounds, compound **6** showed the highest binding affinity (7.4 kcal mol^{-1}) to the active site of NS5B HCV RNA-dependent RNA polymerase. Fig. 3C demonstrated that compound 6 binds within the palm I region, where the phenyl ring makes three H–π interactions with three important amino acid residues (Tyr 415, Met 414 and Cys 366) in addition to two important hydrogen bonds made by NH atom to two key amino acid residues (Tyr 415 and Ser 367). These binding interactions explain the strong binding affinity of compound 6 to the active site of NS5B HCV RNA-dependent RNA polymerase (Table 2).

Compounds **6**, **8** and **12** demonstrated the best binding affinities (−6.7 and −6.9 and −6.9 kcal mol^{-1}, respectively), among the screened compounds, to the active site of NS3/4A protease. Fig. 4C revealed that the phenyl ring of compound **8** binds within protease active site *via* a single H–π interaction with amino acid residue (Lys 1136). This binding interaction elucidates the weak binding affinity of compound **8** to the active site of NS3/4A protease (Table 3). Therefore, NS3/4A HCV protease protein is less likely to be a considerable target for our screened compounds.

As depicted in Fig. 5C, compound **6** binds strongly to the active site of NS3/4A helicase with binding affinity (−7.1 kcal mol^{-1}) very close to the native ligand (−7.7 kcal mol^{-1}). This strong binding affinity could be explained by two reasons. Firstly, compound **6** binds mainly through two strong hydrogen bonds to the key amino acid residues (Asp 496 and Glu 493) as well as a strong ionic bond to Glu 493 (Table 4). Secondly, the alkylamine side chain of compound **6** extended deeply in the lipophilic pocket of helicase active site which also increases the binding affinity of this compound to the target helicase protein. Consequently, NS3/4A helicase protein is more likely to be a potential target for compound **6**, among our screened compounds.

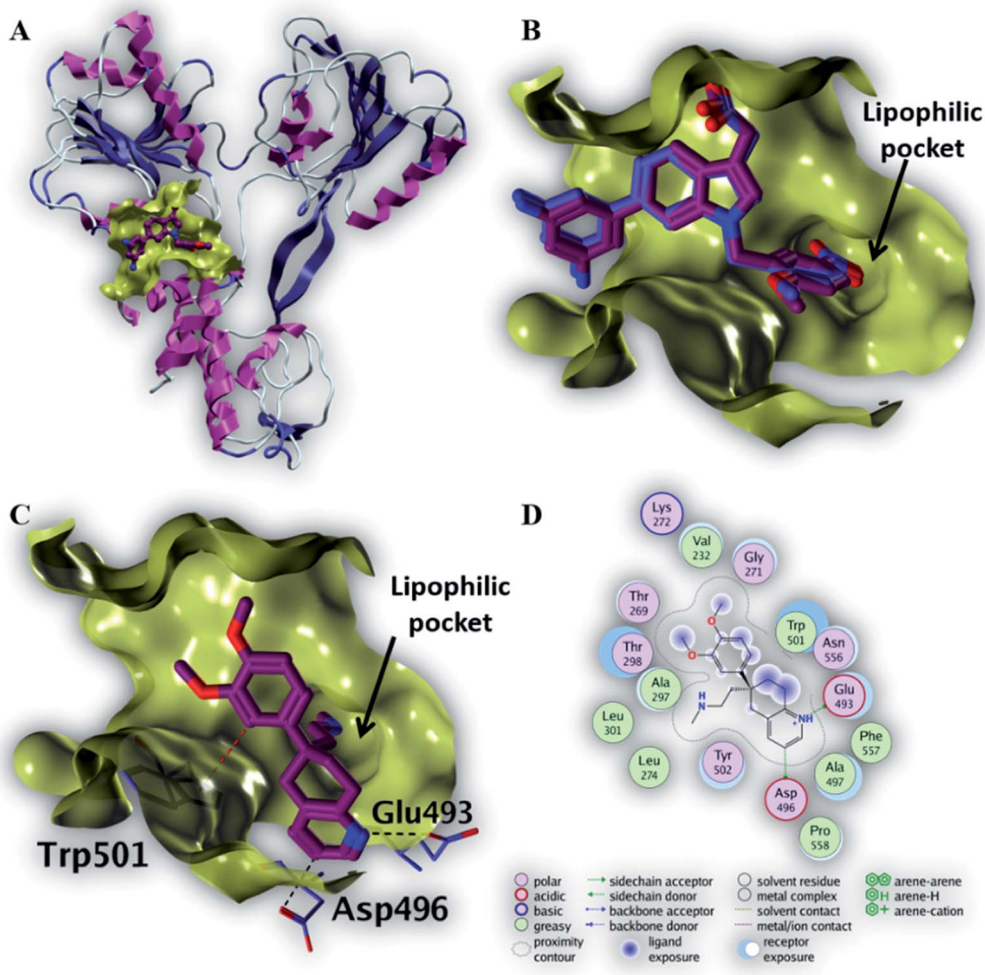

Fig. 5 The top-scoring docked pose of compound **6** to the HCV NS3 helicase active site (PDB code 4OKS) as predicted by MOE 2019.01. (A) An overview of the HCV NS3 helicase active site (B) comparison of modeled binding mode of the co-crystallized ligand (magenta stick model) and its superposed docking conformation (blue stick model). (C) Detailed binding mode of compound **6** (magenta stick model) displaying hydrogen bonds (black dashed line) with the key amino acid residue (blue stick model). (D) 2D depiction of compound **6** binding interactions with the key amino acid residues.

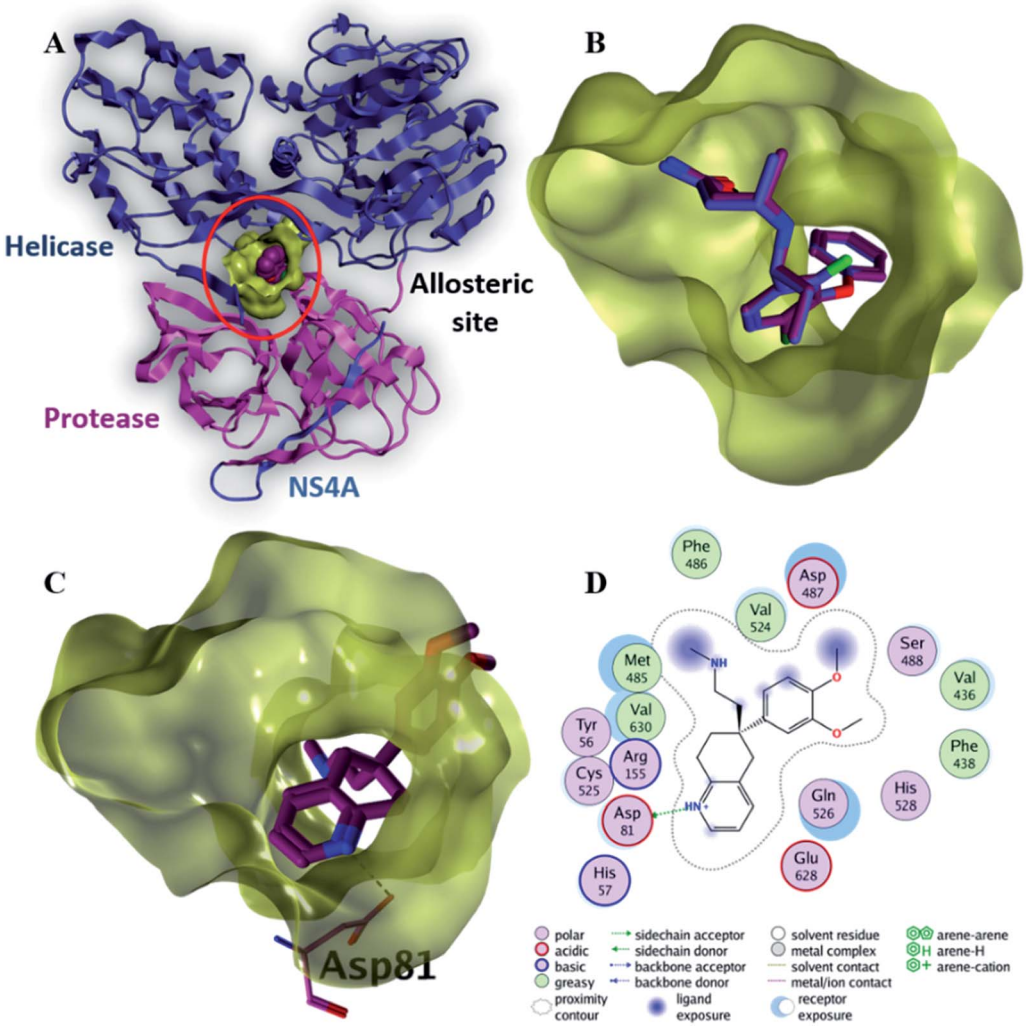

Fig. 6 The top-scoring docked pose of compound **6** to the allosteric site on the HCV NS3–NS4A protein, located between the protease and helicase domains of the HCV NS3 protein (PDB code: 4B73) as predicted by MOE 2019.01. (A) An overview of the allosteric site on the HCV NS3–NS4A protein (B) comparison of modeled binding mode of the co-crystallized ligand (magenta stick model) and its superposed docking conformation (blue stick model). (C) Detailed binding mode of compound **6** (green stick model) displaying hydrogen and ionic bonds (black dashed line) with the key amino acid residue (blue stick model). (D) 2D depiction of compound **6** binding interactions with the key amino acid residue.

Compound **6** displayed the highest binding affinity (-7.9 kcal mol^{-1}) to the allosteric site of the HCV NS3–NS4A protein. As summarized in Table 5, compound **6** binds to the curial amino acid residue Asp 81 forms two bonds, one hydrogen bond and one ionic bond. Fig. 6C and D showed the 3D and 2D depiction of compound **6** within the allosteric site of the HCV NS3–NS4A protein displaying hydrogen and ionic bonds with the key amino acid residue (Asp 81). Subsequently, the new allosteric site of the HCV NS3–NS4A protein is considered as a plausible target for compound **6**.

According to our molecular docking simulation study, compound **6** was the most promising anti-HCV candidate among the twelve members of the alkaloidal fraction of *A. cordifolia* roots as it gives an excellent binding affinity; specifically against NS3/4A helicase and a new allosteric pocket in the HCV NS3–NS4a protein located at the interface between the protease and helicase domains with a relative good binding energy and distance values from the amino acids of the active binding site compared with the native ligands in these proteins.

The ADME analysis has revealed that all the studied compounds show no violations toward Lipinski's rule and hence prove acceptable drug-likeness and pharmacokeintic properties with no potential toxicity (Tables 6 and 7).

3. Material and methods

3.1. Chemicals

All chemicals and solvents were acquired from Merck (Germany) and Sigma Chemical Co. (USA), respectively and were of analytical grades.

3.2. Extraction and isolation

The roots of *A. cordifolia* (250 g) were extracted using 95% ethyl alcohol, the dried ethanol extract (21.5 g) was then suspended

Table 1 The binding affinity of the screened compounds with HCV polymerase, protease, helicase, and protease-helicase allosteric binding site

	Binding affinity ΔG (kcal mol^{-1})			
Ligand	Polymerase	Protease	Helicase	Protease–helicase allosteric
Native ligand (RMSD)	−9.3 (0.28)	−11.3 (0.62)	−7.7 (0.31)	−9.4 (0.16)
1	−5.1	−4.8	−4.7	−5.5
2	−5.1	−4.8	−4.9	−5.7
3	−5.3	−5.0	−5.1	−5.9
4	−6.6	−5.9	−6.5	−7.0
5	−5.2	−4.8	−5.3	−5.7
6	−7.4	−6.7	−7.1	−7.9
7	−6.1	−5.6	−5.7	−6.7
8	−7.1	−6.9	−6.0	−7.4
9	−6.3	−6.4	−5.7	−7.3
10	−6.4	−5.9	−6.0	−7.2
11	−7.1	−6.4	−6.4	−7.1
12	−6.8	−6.9	−6.4	−7.3

in the least amount of distilled water, transferred to separating funnel, then defatted with light petroleum ether to afford pet. ether fraction (3 g). The remaining aqueous solution was then acidified and extracted with ethyl acetate to give acidic ethyl acetate fraction (2.8 g) (non-alkaloidal fraction). The mother liquor was then completely basified and extracted again with ethyl acetate to give basic ethyl acetate fraction (1.8 g) (alkaloidal fraction). The petroleum ether soluble fraction was subjected to silica gel column chromatography and eluted with pet. ether : EtOAc gradient elution starting with 100% pet. ether till 70 : 30 pet. ether : EtOAc to afford four compounds named, capric acid, tricosanol and mixture of β-sitosterol & stigma sterol. Then the acidic EtOAc fraction was subjected to silica gel column chromatography eluted with DCM : MeOH gradient elution to afford five subfractions. Subfraction no. three was further subjected to sephadex LH-20 (Merck, Germany) column chromatography using isocratic elution with DCM : MeOH (50 : 50) to yield *cis-N*-coumaroyl tyramine compound. Finally the alkaloidal fraction was subjected to silica gel column chromatography eluted with DCM : MeOH gradient elution to afford seven subfractions. Subfraction no. 3 was further eluted on sephadex LH-20 (Merck, Germany) column chromatography using isocratic elution with MeOH (100%) to yield compound *O*-methyl sceletenone (**4**), while 4-methoxyphenethylamine (**1**), *N*-methyl tyramine (**2**) and epinine (**5**) compounds were afforded by further purification of subfraction no. 4 on semi preparative HPLC (Knauer, Smartline, Germany) using H_2O/methanol (95 : 5) initially for 5 min, followed by a linear gradient to 100% methanol within 40 min and maintained isocratically for 5 min. Separation was achieved on a preparative C18 column (5 μm, 10 × 250 mm, Waters XBridge, Eschborn, Germany), with a flow rate of 2.0 mL min^{-1} and solvent mixture complemented by 0.05% trifluoroacetic acid.

Table 2 Docking results of the best score compound with HCV NS5B polymerase's active site compared to the native ligand

		Interaction parameters			
Ligand	Binding affinity (ΔG in kcal mol^{-1})	Interaction	AA residue	δ (Å)	E (kcal mol^{-1})
Native ligand	−9.3	H-Donor	Asp 318 (side chain)	2.71	−7.2
		H-Acceptor	Ser 556 (side chain)	3.11	−1.0
		H-Acceptor	Asn 291 (side chain)	2.88	−3.5
		H–π	Met 414 (side chain)	4.77	−0.5
6	−7.4	H-Donor	Tyr 415 (side chain)	3.10	−0.2
		H-Acceptor	Ser 367 (side chain)	3.40	−0.2
		H–π	Tyr 415 (side chain)	4.59	−0.6
		H–π	Met 414 (side chain)	4.81	−0.3
		H–π	Cys 366 (side chain)	4.23	−0.2

Table 3 Docking results of the best score compound with the active site of HCV NS3-4a protease compared to the native ligand

		Interaction parameters			
Ligand	Binding affinity (ΔG in kcal mol^{-1})	Interaction	AA residue	δ (Å)	E (kcal mol^{-1})
Native ligand	−11.3	H-Donor	Arg 1155 (backbone)	2.82	−4.6
		H-Donor	His 1057 (side chain)	3.01	−7.5
		H-Donor	Ala 1157 (backbone)	2.88	−4.3
		H-Acceptor	Gly 1137 (backbone)	3.00	−1.1
		H-Acceptor	Gly 1137 (backbone)	3.02	−2.8
		H-Acceptor	Ala 1157 (backbone)	2.95	−3.7
		H–π	His 1057 (side chain)	3.68	−1.6
8	−6.9	H–π	Lys 1136 (side chain)	4.36	−0.6

Table 4 Docking results of the best score compound with the active site of HCV helicase compared to the native ligand

		Interaction parameters			
Ligand	Binding affinity (ΔG in kcal mol^{-1})	Interaction	AA residue	δ (Å)	E (kcal mol^{-1})
Native ligand	−7.7	H-Donor	Trp 501 (backbone)	2.81	−2.3
		H-Acceptor	Gly 255 (backbone)	2.91	−3.5
		H-Acceptor	Gly 255 (backbone)	2.92	−4.6
		H-Acceptor	Thr 269 (side chain)	3.52	−1.9
6	−7.1	H-Donor	Asp 496 (side chain)	3.35	−0.7
		H-Donor	Glu 493 (side chain)	2.91	−13.1
		Ionic	Glu 493 (side chain)	2.91	−5.1

Table 5 Docking results of the best score compound with the active site of HCV protease-helicase allosteric site compared to the native ligand

		Interaction parameters			
Ligand	Binding affinity (ΔG in kcal mol^{-1})	Interaction	AA residue	δ (Å)	E (kcal mol^{-1})
Native ligand	−9.4	H-Donor	Asp 79 (backbone)	3.46	−0.7
		H-Donor	Cys 525 (backbone)	3.00	−4.2
		H-Donor	H_2O (glu 628)	3.04	−5.3
		H-Donor	Leu 517 (backbone)	2.99	−1.1
		H-Acceptor	Cys 525 (backbone)	2.97	−4.8
6	−7.9	H-Donor	Asp 81 (side chain)	2.97	−4.9
		Ionic	Asp 81 (side chain)	3.47	−2.0

Table 6 Drug-likeness based on Lipinski's rule of five, TPSA and number of rotatable bonds

Molecule	Hydrogen bond donors	Hydrogen bond acceptors	Number of rotatable bonds	M log P	Molecular weight	Number of violations
1	1	2	3	1.53	151.21	0
2	2	2	3	1.53	151.21	0
3	1	2	3	1.83	165.23	0
4	0	3	2	2.00	257.33	0
5	3	3	3	0.92	167.21	0
6	1	4	6	2.27	326.44	0
7	1	3	1	1.75	243.31	0
8	0	3	3	2.68	275.39	0
9	0	3	2	2.08	259.35	0
10	1	3	4	2.08	261.37	0
11	0	3	5	2.24	273.38	0
12	0	3	5	2.33	275.39	0

3.3. Antiviral activity

HCV replicon cells were inoculated at 26×10^4 cells per well in a 48-well plate for 24 h prior to the experiment. Each investigated fraction (petroleum ether, acidic ethyl acetate and basic ethyl acetate) was added to the culture broth at different concentrations (1–200 μg mL^{-1}). After 72 h, the treated cells were harvested and lysed in cell culture lysis reagent. Luciferase activity was evaluated with a luciferase assay system and the resulting luminescence was detected by the luminescence plate reader (PerkinElmer) and corresponded to the expression level of the HCV replicon. MTT assay was used to monitor the cytotoxicity which could be attributed to some compounds in the extracts.

3.4. Molecular docking

Molecular operating environment software (MOE 2019.01, Chemical Computing Group, Montreal, QC, Canada) was used to perform all the docking algorithms in this study in addition to ranking and visualization of the generated docking poses. Four co-crystal structures (PDB ID: 3H2L, 6NZT, 4OKS, 4B73) [10.1016/j.bmcl.2009.09.045, 10.1016/j.bmcl.2019.03.037, 10.1021/jm401432c, 10.1038/nchembio.1081], which represent the four non-structural HCV targets, were retrieved from the protein data bank and involved in our molecular docking simulation. All protein structures were prepared by QuickPrep module implemented in MOE before docking. The chemical structures of the screened compounds were drawn and energy

Table 7 ADMET and medicinal chemistry properties of isolated as well as dereplicated compounds

Molecule	Bioavilability score	GI absorption	BBB permeation	Pgp substrate	PAINS alerts	Synthetic accessibility
1	0.55	High	Yes	No	0	1.00
2	0.55	High	Yes	No	0	1.00
3	0.55	High	Yes	No	0	1.00
4	0.55	High	Yes	No	0	3.32
5	0.55	High	Yes	No	1, catechol	1.09
6	0.55	High	Yes	Yes	0	3.32
7	0.55	High	Yes	No	0	3.25
8	0.55	High	Yes	No	0	2.99
9	0.55	High	Yes	No	0	2.66
10	0.55	High	Yes	No	0	1.80
11	0.55	High	Yes	No	0	3.02
12	0.55	High	Yes	No	0	1.95

minimized by MOE default settings. MOE induced docking protocol was applied, where the co-crystallized ligand was used as a center for the docking simulation grid. All water molecules as well as other non-essential ligands were removed before docking. Other parameters were left in their default value.

3.5. *In silico* drug-likeness, ADME profiling, and toxicity risk assessment

The drug-likeness and pharmacokinetic properties of all identified compounds were predicted using Swiss ADME database.[36]

4. Conclusion

The investigation of *A. cordifolia* roots revealed isolation and structure elucidation of eight compounds. Additionally, the alkaloidal fraction showed potent anti HCV activity with IC_{50} value of 2.4 μg mL^{-1} so, we undergo docking studies of compounds isolated from alkaloidal fraction as well as, alkaloidal compounds dereplicated from the same fraction through metabolomics. The structure-based screening of the compounds was elucidated against four non-structural HCV antiviral targets and revealed that tortuosamine compound could be a promising anti-HCV candidate as it showed the strongest binding to the active site of NS3/4A helicase among the others. Accordingly, our *in silico* study highlights the importance of the alkaloidal fraction of the *A. cordifolia* roots as a potential complementary remedy for HCV infections after further validation.

Conflicts of interest

There are no conflicts to declare.

Acknowledgements

This publication was funded by Minia University.

References

1 Q.-L. Choo, G. Kuo, A. J. Weiner, L. R. Overby, D. W. Bradley and M. Houghton, *Science*, 1989, **244**, 359–362.
2 R. De Francesco, L. Tomei, S. Altamura, V. Summa and G. Migliaccio, *Antiviral Res.*, 2003, **58**, 1–16.
3 S. T. Hassan, K. Berchová-Bímová and J. Petráš, *Phytother. Res.*, 2016, **30**, 1487–1492.
4 G. Hussein, H. Miyashiro, N. Nakamura, M. Hattori, N. Kakiuchi and K. Shimotohno, *Phytother. Res.*, 2000, **14**, 510–516.
5 A. Petruzziello, S. Marigliano, G. Loquercio, A. Cozzolino and C. Cacciapuoti, *World J. Gastroenterol.*, 2016, **22**, 7824.
6 A. A. Youssef, N. Magdy, L. A. Hussein and A. El-Kosasy, *J. Chromatogr. Sci.*, 2019, **57**, 636–643.
7 D. L. Wyles and A. F. Luetkemeyer, *Top. Antivir. Med.*, 2017, **25**, 103.
8 M. Debiaggi, L. Pagani, P. Cereda, P. Landini and E. Romero, *Microbiologica*, 1988, **11**, 55–61.
9 K. Asres and F. Bucar, *Ethiop. Med. J.*, 2005, **43**, 15–20.
10 K. Vermani and S. Garg, *J. Ethnopharmacol.*, 2002, **80**, 49–66.
11 K.-L. Huang, Y.-K. Lai, C.-C. Lin and J.-M. Chang, *World J. Gastroenterol.*, 2006, **12**, 5721.
12 D. H. Kwon, H. Y. Kwon, H. J. Kim, E. J. Chang, M. B. Kim, S. K. Yoon, E. Y. Song, D. Y. Yoon, Y. H. Lee and I. S. Choi, *Phytother. Res.*, 2005, **19**, 355–358.
13 G. J. Kotwal, J. N. Kaczmarek, S. Leivers, Y. T. Ghebremariam, A. P. Kulkarni, G. Bauer, C. De Beer, W. Preiser and A. R. Mohamed, *Ann. N. Y. Acad. Sci.*, 2005, **1056**, 293–302.
14 M. Musarra-Pizzo, R. Pennisi, I. Ben-Amor, G. Mandalari and M. T. Sciortino, *Viruses*, 2021, **13**, 828.
15 T. B. N. Trinh, D. H. Le, T. T. K. Nguyen, M. H. Nguyen, M. Muller and T. K. N. Nguyen, *Virusdisease*, 2021, 1–7.
16 T. S. Wahyuni, A. A. Permatasari, T. Widiandani, A. Fuad, A. Widyawaruyanti, C. Aoki-Utsubo and H. Hotta, *Nat. Prod. Commun.*, 2018, **13**, 1579–1582.
17 G. Germishuizen and N. Meyer, *Plants of southern Africa: an annotated checklist*, National Botanical Institute Pretoria, 2003.

18 Mifsud S (2002–2014), MaltaWildPlants.com – an online flora of the Maltese islands, Accessed 20 Nov 2018, http://www.maltawildplants.com.
19 A. A. E. Said, T. F. Ali, E. Z. Attia, A.-S. F. Ahmed, A. H. Shehata, U. R. Abdelmohsen and M. A. Fouad, *Nat. Prod. Res.*, 2020, 1–5.
20 D. Elgindi and T. Mabry, *Asian J. Chem.*, 1999, **11**, 1525.
21 S. Sultana, M. Ali and S. R. Mir, *Int. J. Adv. Pharm. Med. Bioallied Sci.*, 2017, **5**, 217–224.
22 B. Silva Ferreira, L. Pereira Faza and M. Le Hyaric, *Sci. World J.*, 2012, **2012**, 1–4.
23 D. K. Kim, J. P. Lim, J. W. Kim, H. W. Park and J. S. Eun, *Arch. Pharm. Res*, 2005, **28**, 39–43.
24 N. Hiroka and D. P. Carew, *J. Nat. Prod.*, 1981, **44**, 285–288.
25 K. K. Hornemann, J. Neal and J. McLaughlin, *J. Pharm. Sci.*, 1972, **61**, 41–45.
26 H. Sato, S. Sakamura and Y. Obata, *Agric. Biol. Chem.*, 1970, **34**, 1254–1255.
27 P. W. Jeffs, T. Capps, D. Johnson, J. Karle, N. Martin and B. Rauckman, *J. Org. Chem.*, 1974, **39**, 2703–2710.
28 C. D. Gaffney, PhD thesis, University of Johannesburg, South Africa, 2008.
29 R. J. Borgman, J. J. McPhillips, R. E. Stitzel and I. J. Goodman, *J. Med. Chem.*, 1973, **16**, 630–633.
30 C. G. Chavdarian, D. Karashima, N. Castagnoli Jr and H. K. Hundley, *J. Med. Chem.*, 1978, **21**, 548–554.
31 T. A. Smith, *Phytochemistry*, 1977, **16**, 9–18.
32 P. Halfon and S. Locarnini, *J. Hepatol.*, 2011, **55**, 192–206.
33 B. Nutho, W. Khuntawee, C. Rungnim, P. Pongsawasdi, P. Wolschann, A. Karpfen, N. Kungwan and T. Rungrotmongkol, *Beilstein J. Org. Chem.*, 2014, **10**, 2789–2799.
34 A. H. Al-Saeedi, M. T. H. Al- Ghafri and M. A. Hossain, *Pac. Sci. Rev.*, 2016, **18**, 78–83.
35 C. M. Rice, *Top. Antivir. Med.*, 2011, **19**, 117.
36 A. Daina, O. Michielin and V. Zoete, *Sci. Rep.*, 2017, **7**, 1–13.